

## Supporting information

### Cooperative B-site octahedral tilting, distortion and A-site conformational change induced phase transition of 2D Lead Halide Perovskite

Muhammad Azeem,<sup>a</sup> Yan Qin,<sup>b</sup> Zhi-Gang Li,<sup>a</sup> Wei Li,<sup>\*a</sup>

a. School of Materials Science and Engineering, Nankai University, Tianjin 300350, China

b. School of Physics and Wuhan National Laboratory for Optoelectronics, Huazhong University of Science and Technology, Wuhan 430074, China

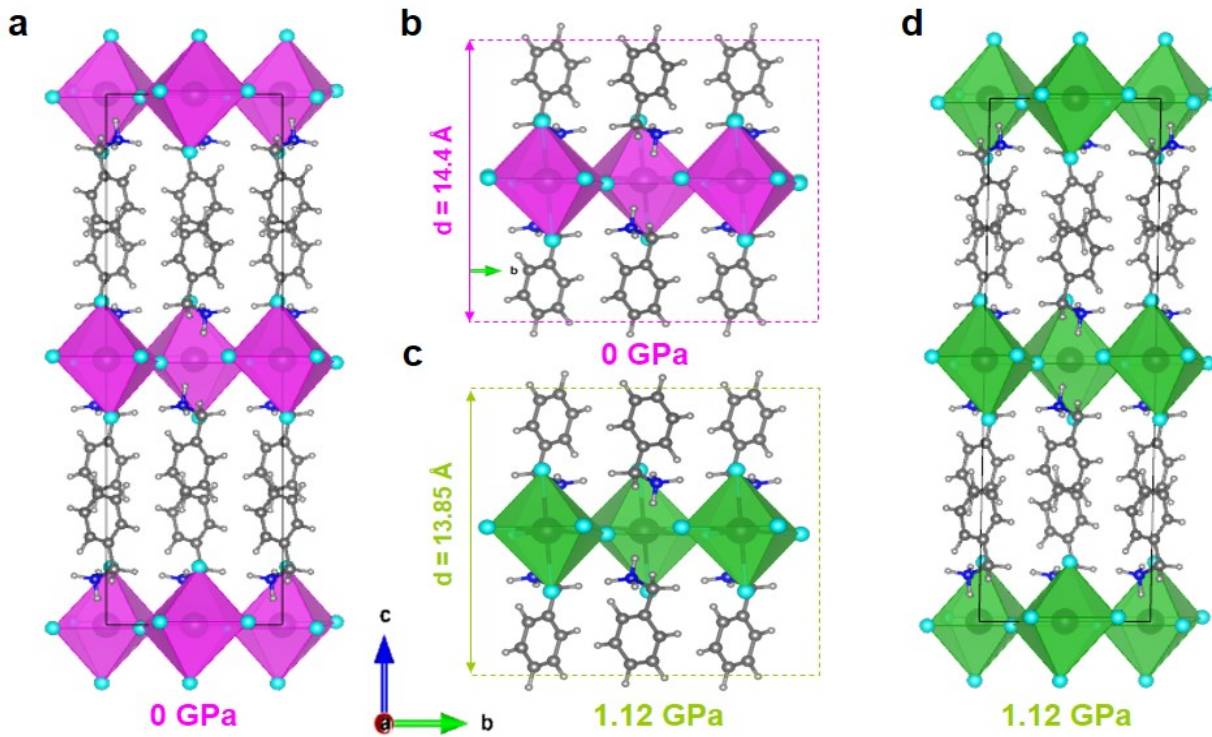


**Fig. S1.** Structure and layer thickness of  $(\text{BA})_2\text{PbI}_4$  at low pressure phase (pink octahedra at 0 GPa) and at high pressure phase (green octahedra at 1.12 GPa). (a, d) Inorganic layer sandwich between two organic layers stacked along  $c$ -axis in a unit cell. (b, c) The layer thickness is about 14.4 Å at 0 GPa, and 13.85 Å at 1.12 GPa.

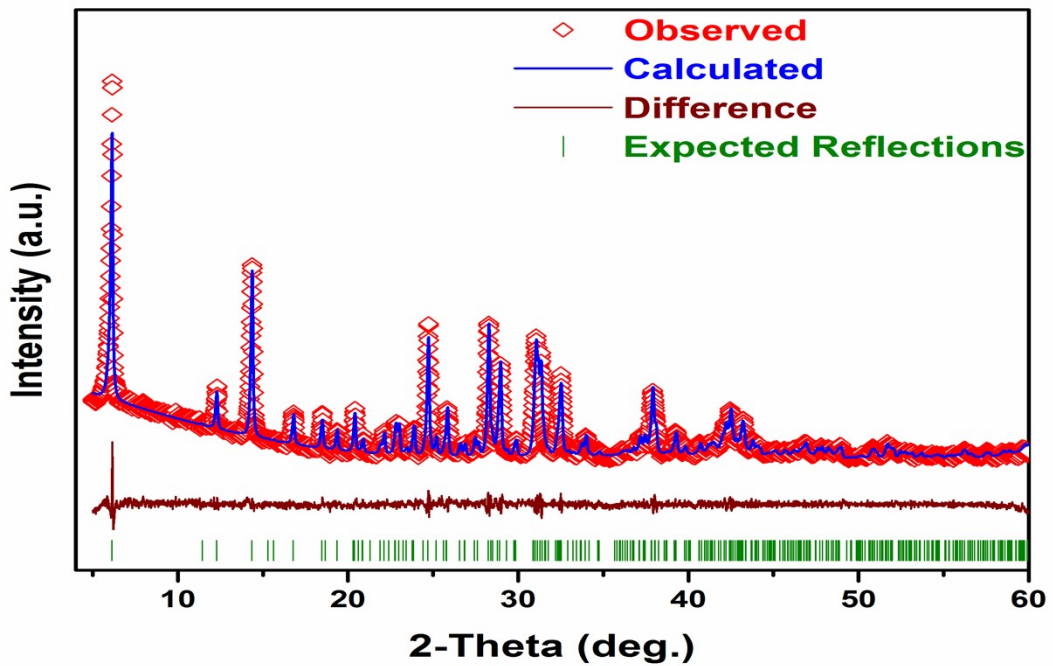


**Fig. S2.** Le-Bail refinements of  $(\text{BA})_2\text{PbI}_4$  at ambient pressure in Phase-I (orthorhombic “ $Pbca$ ”).

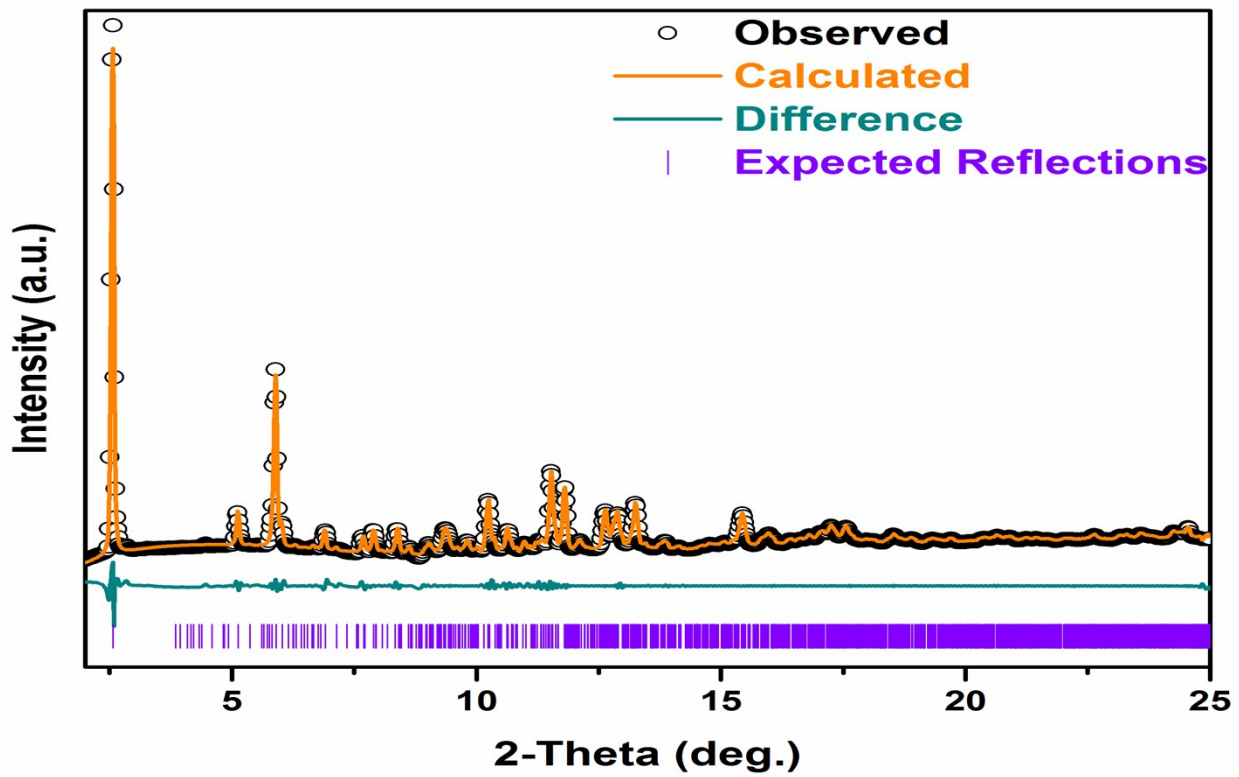


**Fig. S3.** Le-Bail refinements of  $(BA)_2PbI_4$  at 1.12 GPa pressure in Phase-II (triclinic “*P*-I”).

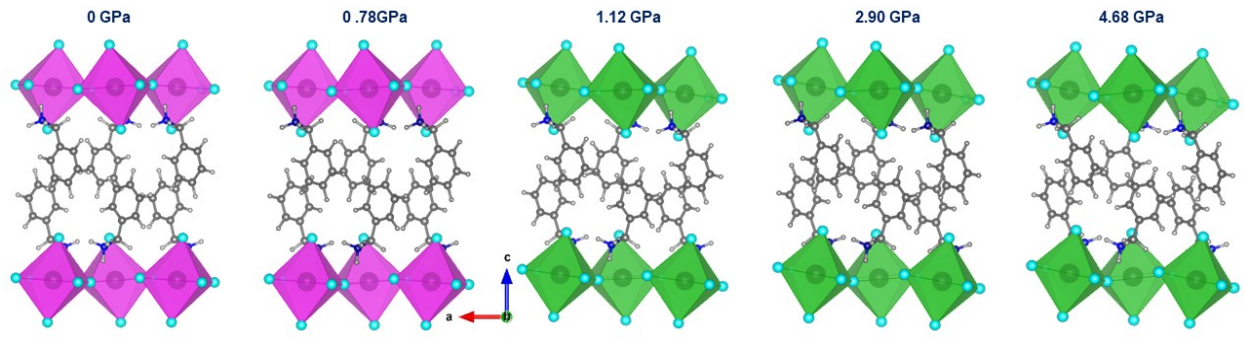


**Fig. S4.** The molecular structure of  $(BA)_2PbI_4$ , the conformation of BA cations, and  $(PbI_4)^{2-}$  inorganic unit in *ac*-direction at different pressures.

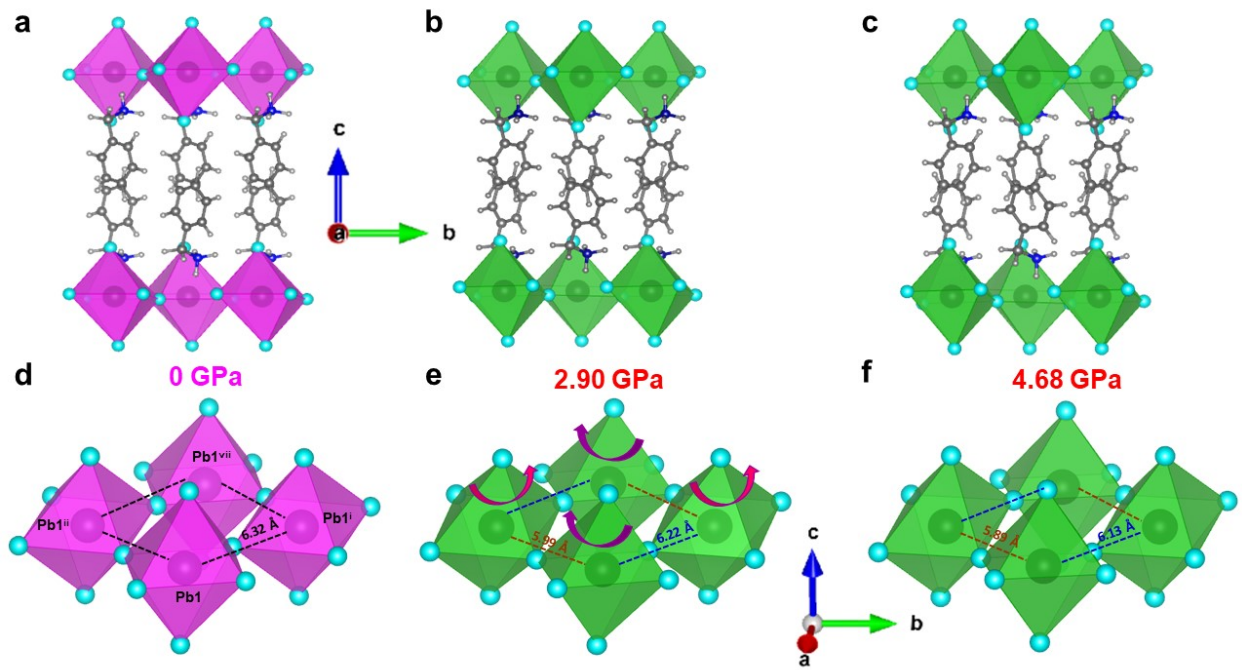


**Fig. S5.** The structure of  $(\text{BA})_2\text{PbI}_4$ , the conformation of BA cations, and  $(\text{PbI}_4)^{2-}$ -inorganic unit, at 0 GPa [a and d], 2.9 GPa [b and e], and 4.68 GPa [c and f], while [a-c] are in  $bc$ -direction showing layer stacking, while [d-f] indicating  $\text{PbI}_6$  octahedra at unit cell edges with distortion in different directions. Obtained by experiment-aided DFT calculations. Symmetry codes: (i) 0.5-x, -y, 0.5+z; (ii) 0.5-x, 1-y, 0.5+z; (iii) -0.5+x, y, 1.5-z; (iv) x, 0.5-y, 0.5+z; (v) 0.5+x, y, 1.5-z; (vi) -x, -0.5+y, 1.5-z; (vii) 1-x, 0.5+y, 1.5-z.

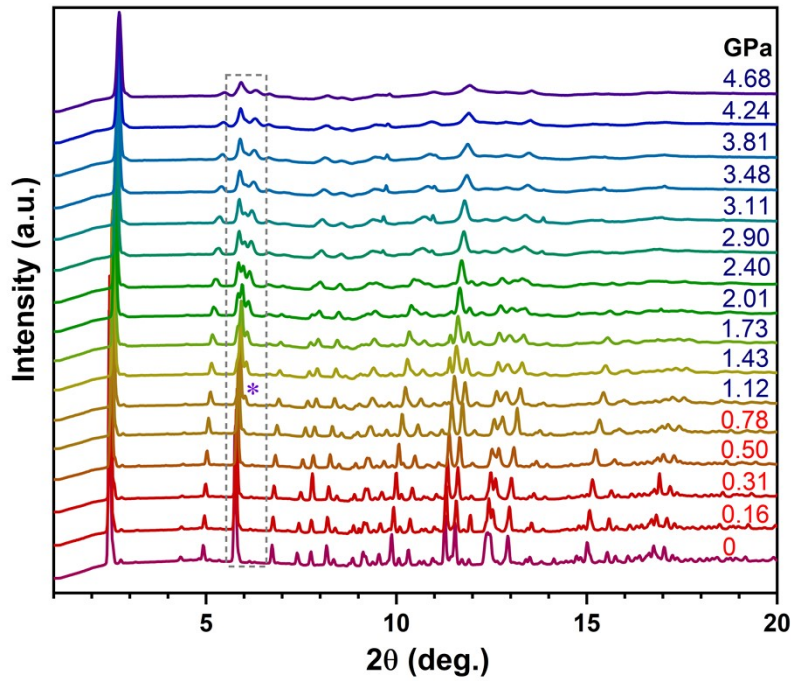


**Fig. S6.** High-pressure evolution of  $(\text{BA})_2\text{PbI}_4$  single crystal. XRD patterns from ambient to 4.68 GPa. XRD patterns of Phase-I and Phase-II with a new peak at about  $6.02^\circ$ .

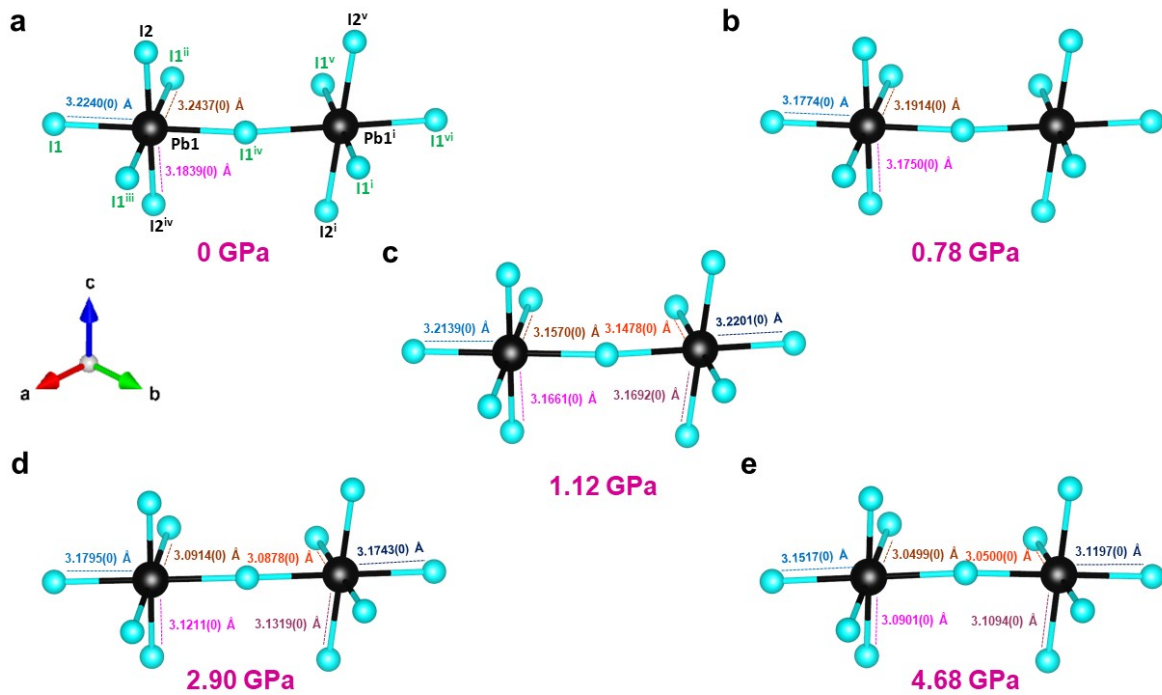


**Fig. S7.** The bond lengths within the two adjacent  $\text{PbI}_6$  octahedra at different pressure at; (a) 0 GPa (b) 0.78 GPa (c) 1.12 GPa, (d) 2.90 GPa, and (e) 4.68 GPa, obtained by experiment-aided DFT calculations. Symmetry codes: (i) 0.5-x, -y, 0.5+z; (ii) 0.5-x, 1-y, 0.5+z; (iii) -0.5+x, y, 1.5-z; (iv) x, 0.5-y, 0.5+z; (v) 0.5+x, y, 1.5-z; (vi) -x, -0.5+y, 1.5-z; (vii) 1-x, 0.5+y, 1.5-z.

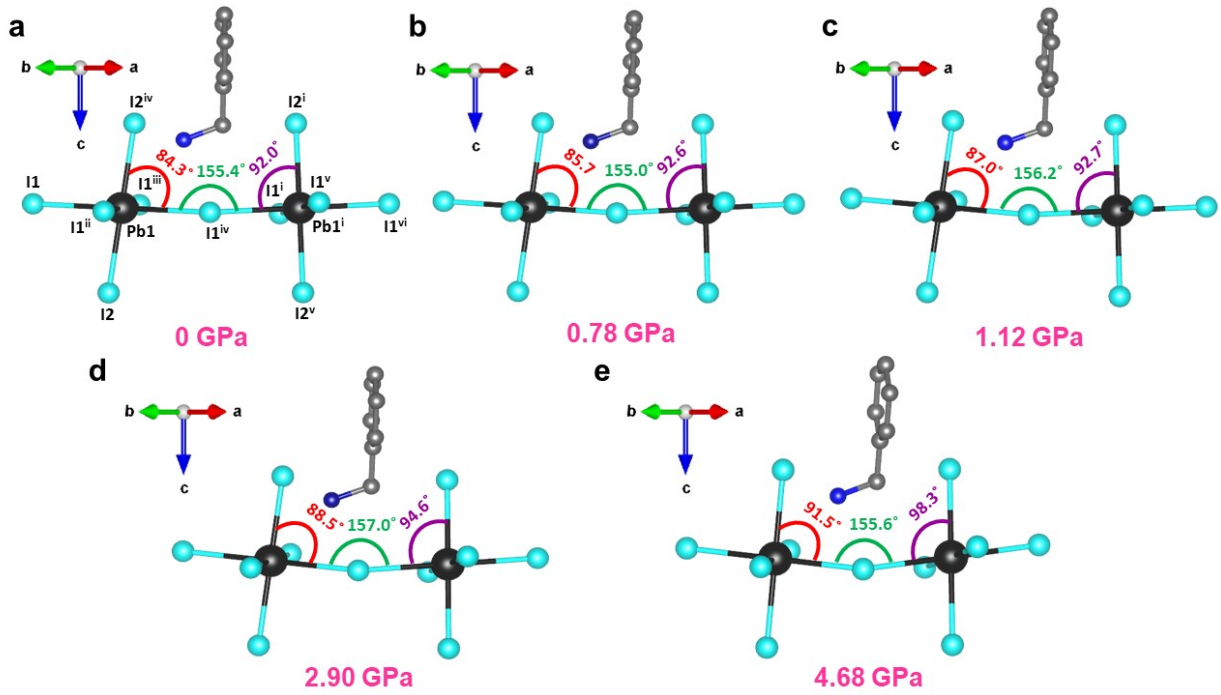


**Fig. S8.** The tilting of two adjacent  $\text{PbI}_6$  octahedra under different pressure. Symmetry codes: (i) 0.5-x, -y, 0.5+z; (ii) 0.5-x, 1-y, 0.5+z; (iii) -0.5+x, y, 1.5-z; (iv) x, 0.5-y, 0.5+z; (v) 0.5+x, y, 1.5-z; (vi) -x, -0.5+y, 1.5-z; (vii) 1-x, 0.5+y, 1.5-z.

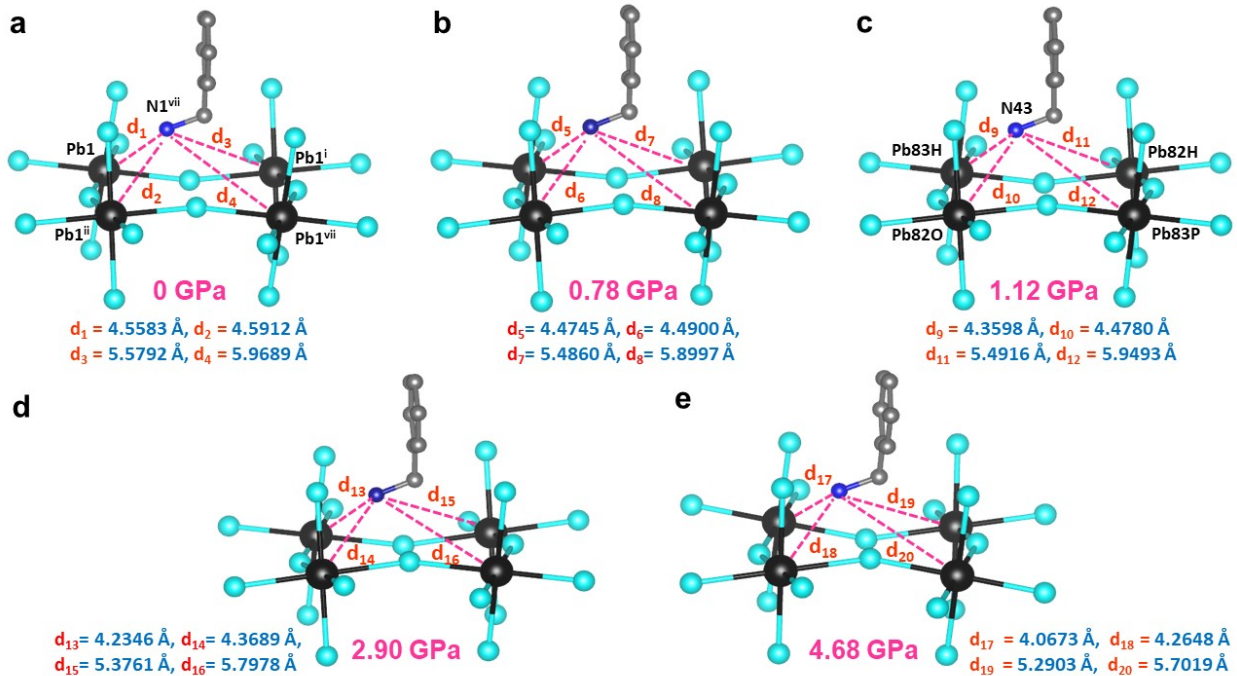


**Fig. S9.** The distance of nitrogen atom from Pb atoms at; (a) 0 GPa (b) 0.78 GPa (c) 1.12 GPa, (d) 2.90 GPa, and (e) 4.68 GPa. Symmetry codes: (i) 0.5-x, -y, 0.5+z; (ii) 0.5-x, 1-y, 0.5+z; (iii) -0.5+x, y, 1.5-z; (iv) x, 0.5-y, 0.5+z; (v) 0.5+x, y, 1.5-z; (vi) -x, -0.5+y, 1.5-z; (vii) 1-x, 0.5+y, 1.5-z.

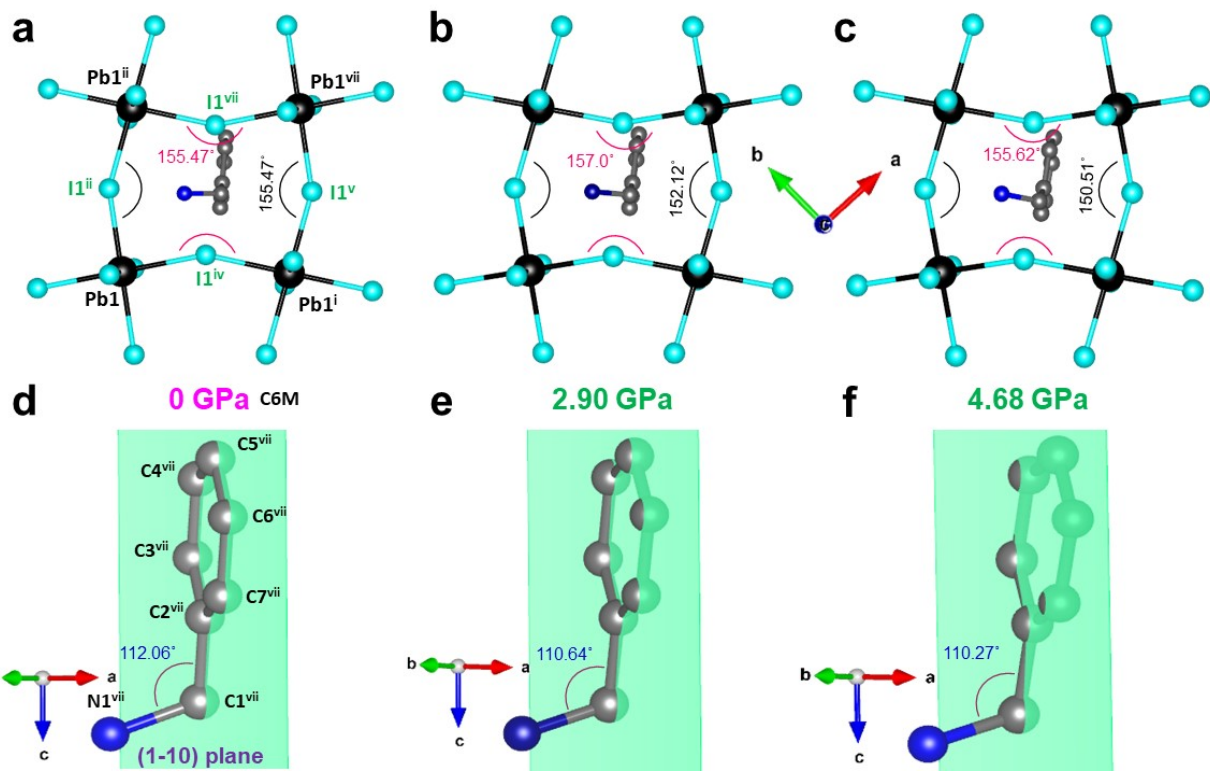


**Fig. S10.** The tilting distortion of  $\text{PbI}_6$  octahedra and configurational changes in of  $\text{BA}^+$  cation at 0.78 GPa (a), and at 2.9 GPa (b) obtained by experiment-aided DFT calculations. Hydrogen atoms are removed for clarity. Symmetry codes: (i)  $0.5-x$ ,  $-y$ ,  $0.5+z$ ; (ii)  $0.5-x$ ,  $1-y$ ,  $0.5+z$ ; (iii)  $-0.5+x$ ,  $y$ ,  $1.5-z$ ; (iv)  $x$ ,  $0.5-y$ ,  $0.5+z$ ; (v)  $0.5+x$ ,  $y$ ,  $1.5-z$ ; (vi)  $-x$ ,  $-0.5+y$ ,  $1.5-z$ ; (vii)  $1-x$ ,  $0.5+y$ ,  $1.5-z$ .

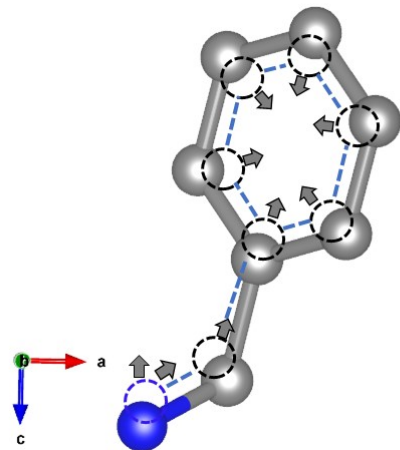


**Fig. S11.** General configurational behavior in of  $\text{BA}^+$  cation under pressure. Hydrogen atoms are removed for clarity

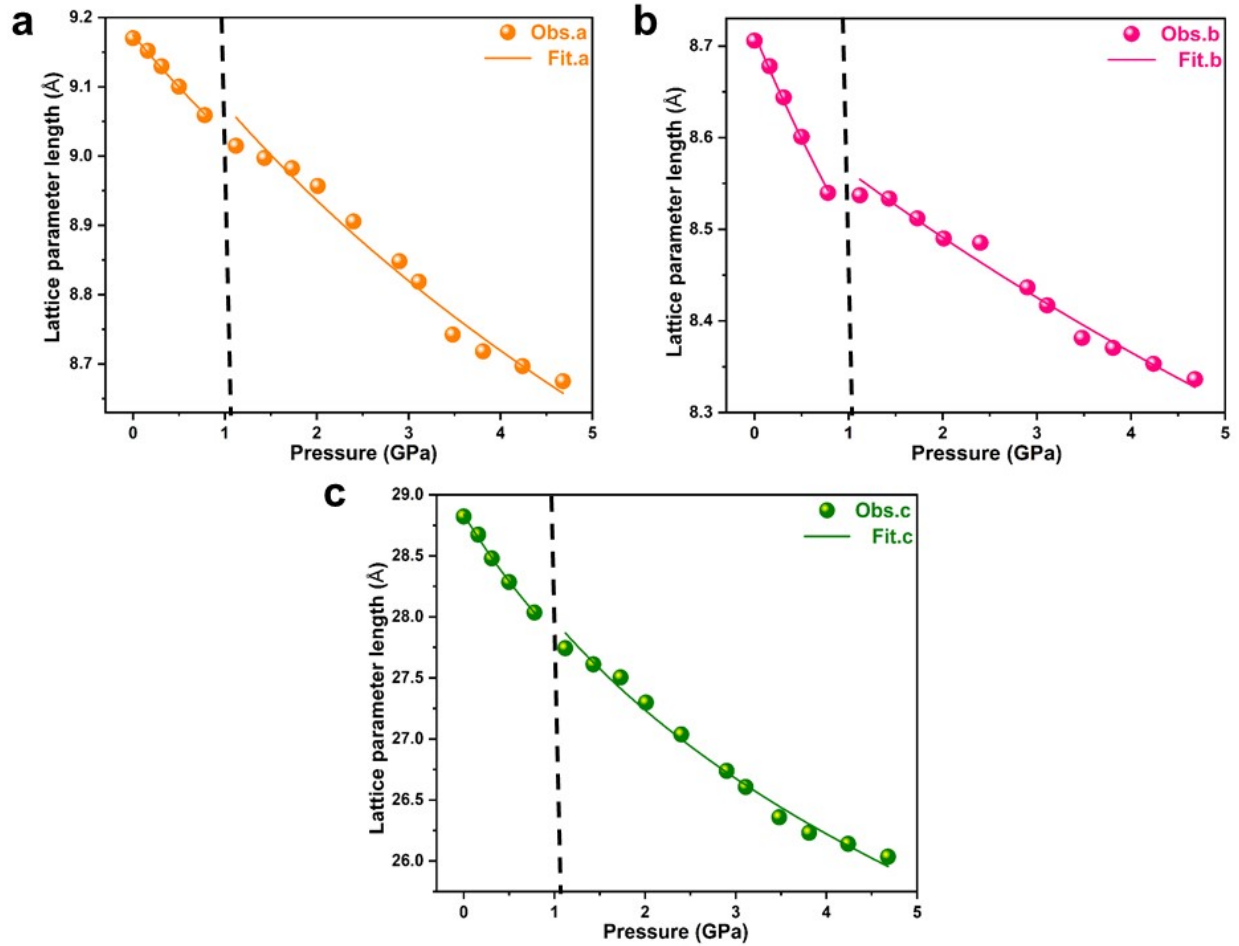


**Fig. S12.** The evolution of lattice parameters as a function of pressure, fitted by Second-order Birch-Murnaghan EoS using PASCal software. (a) Lattice parameter ‘*a*’ (b) lattice parameter ‘*b*’ (c) lattice parameter ‘*c*’.

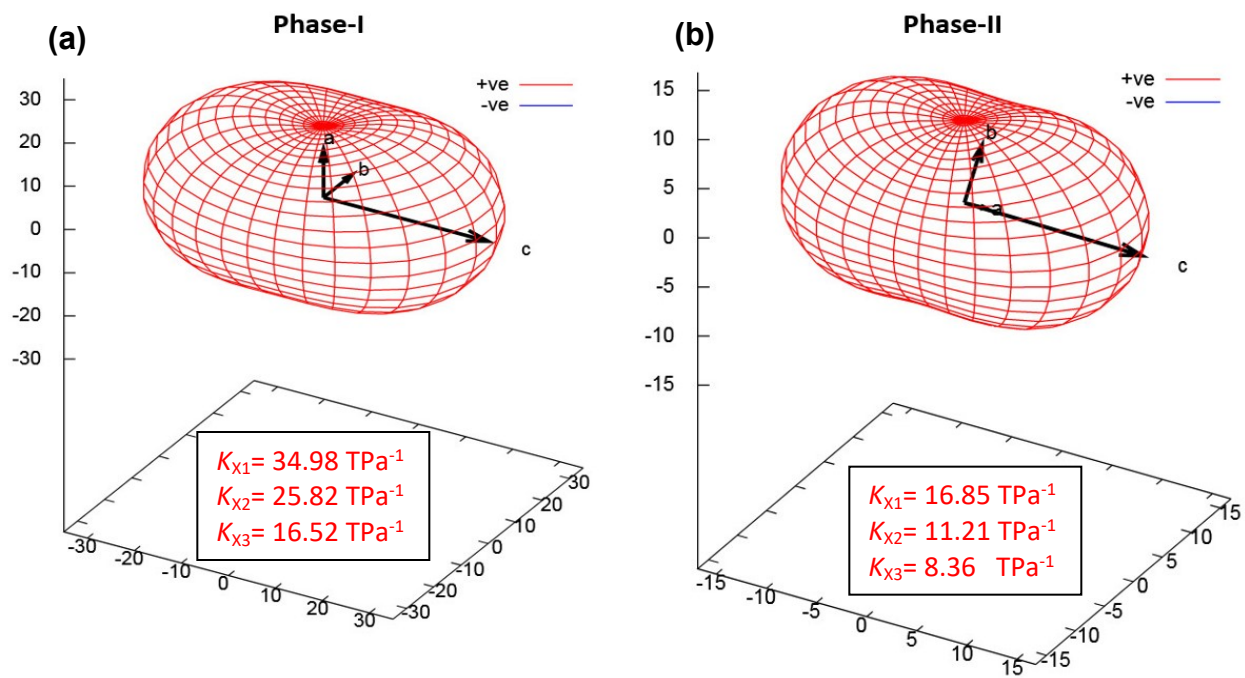


**Fig. S13.** The linear compressibility indicatrices along three orthogonal directions for two phases.

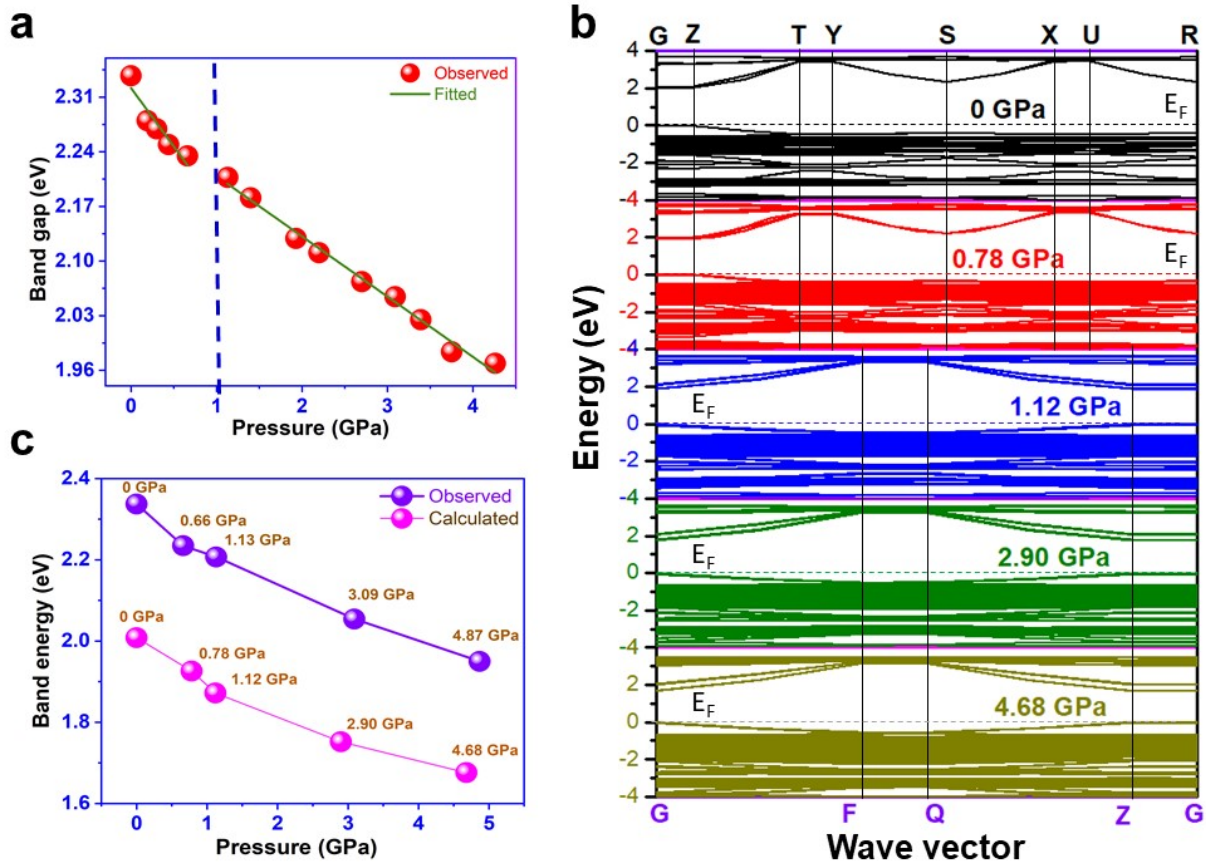


**Fig. S14.** The band energy behavior as a function of pressure (compression) (a) Band energy reduction under pressure. (b) Band energy comparison at different pressures (observed and calculated). (c) Band energy calculations via DFT at different pressures.

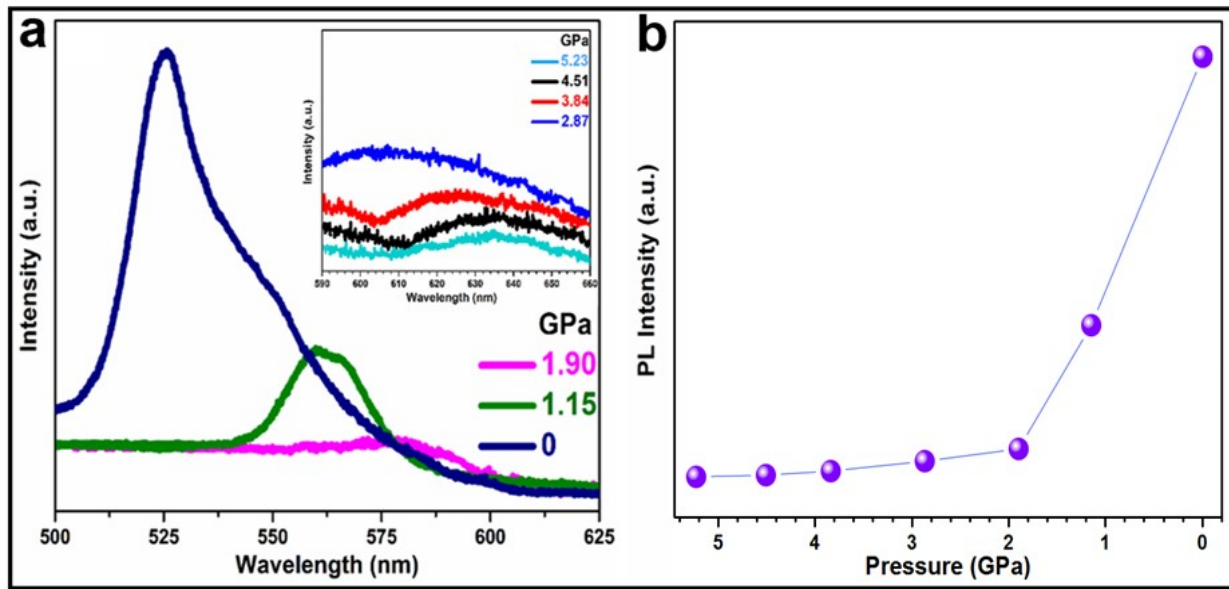


**Fig. S15.** The PL behavior as a function of pressure (decompression) (a) PL spectra ( $1.90\text{ GPa} \rightarrow 0\text{ GPa}$ ), inset showed the recovery of enhanced nonradioactive process induced by amorphization ( $5.23 \rightarrow 2.87\text{ GPa}$ ). (b) PL intensity evolution with decompression.

**Table S1.** Calculated bond lengths and angles for PbI<sub>6</sub> octahedra at different pressures in Phase-I and Phase-II. Symmetry codes: Symmetry codes: (i) 0.5-x, -y, 0.5+z; (ii) 0.5-x, 1-y, 0.5+z; (iii) -0.5+x, y, 1.5-z; (iv) x, 0.5-y, 0.5+z; (v) 0.5+x, y, 1.5-z; (vi) -x, -0.5+y, 1.5-z; (vii) 1-x, 0.5+y, 1.5-z.

Distance (Å)	Phase-I		Phase-II		
	0 GPa	0.78 GPa	1.12 GPa	2.90 GPa	4.68 GPa
Pb1–I2 <sup>iv</sup>	3.1814	3.1750	3.1692	3.1319	3.1095
Pb1–I1 <sup>iv</sup>	3.2437	3.1915	3.2201	3.1744	3.1197
Pb1–I1 <sup>ii</sup>	3.2241	3.1775	3.1478	3.0879	3.0500
Pb1–I2	3.1814	3.1750	3.1692	3.1319	3.1095
Pb1–I1	3.2437	3.1915	3.2201	3.1744	3.1197
Pb1–I1 <sup>iii</sup>	3.2241	3.1775	3.1478	3.0879	3.0500
Pb1 <sup>i</sup> –I2 <sup>i</sup>	3.1814	3.1750	3.1661	3.1212	3.0901
Pb1 <sup>i</sup> –I1 <sup>iv</sup>	3.2241	3.1775	3.2139	3.1795	3.1517
Pb1 <sup>i</sup> –I1 <sup>v</sup>	3.2437	3.1915	3.1570	3.0914	3.0500
Pb1 <sup>i</sup> –I2 <sup>v</sup>	3.1814	3.1750	3.1661	3.1212	3.0901
Pb1 <sup>i</sup> –I1 <sup>vi</sup>	3.2241	3.1775	3.2139	3.1795	3.1517
Pb1 <sup>i</sup> –I1 <sup>i</sup>	3.2437	3.1915	3.1570	3.0914	3.0500
Pb1–Pb1 <sup>i</sup>	6.3202	6.2182	6.2959	6.2264	6.1301
Pb1 <sup>i</sup> –Pb1 <sup>vii</sup>	6.3202	6.2182	6.1186	5.9973	5.8991
Pb1 <sup>vii</sup> –Pb1 <sup>ii</sup>	6.3202	6.2182	6.2959	6.2264	6.1301
Pb1 <sup>ii</sup> –Pb1	6.3202	6.2182	6.1186	5.9973	5.8991

Angle (°)	Phase-I		Phase-II		
	0 GPa	0.78 GPa	1.12 GPa	2.90 GPa	4.68 GPa
$\angle \text{Pb1-I1}^{\text{iv}}-\text{Pb1}^{\text{i}}$	155.473	155.020	156.213	157.008	155.623
$\angle \text{Pb1-I1}^{\text{ii}}-\text{Pb1}^{\text{ii}}$	155.473	155.020	152.075	152.117	150.510
$\angle \text{Pb1}^{\text{ii}}-\text{I1}^{\text{vii}}-\text{Pb1}^{\text{vii}}$	155.473	155.020	156.213	157.008	155.623
$\angle \text{Pb1}^{\text{vii}}-\text{I1}^{\text{v}}-\text{Pb1}^{\text{i}}$	155.473	155.020	152.075	152.117	150.510
$\angle \text{I2}^{\text{iv}}-\text{Pb1}-\text{I1}^{\text{iv}}$	84.306	85.772	87.097	88.566	91.496
$\angle \text{I2}^{\text{iv}}-\text{Pb1}-\text{I1}^{\text{ii}}$	92.053	92.626	94.608	95.551	95.910
$\angle \text{I2}^{\text{i}}-\text{Pb1}^{\text{i}}-\text{I1}^{\text{iv}}$	92.053	92.626	92.724	94.598	98.290
$\angle \text{I2}^{\text{i}}-\text{Pb1}^{\text{i}}-\text{I1}^{\text{v}}$	95.694	94.228	94.581	92.861	90.913
$\angle \text{I1}^{\text{ii}}-\text{Pb1}-\text{I1}^{\text{iv}}$	86.915	86.450	88.831	89.467	90.649
$\angle \text{I1}^{\text{iv}}-\text{Pb1}^{\text{i}}-\text{I1}^{\text{v}}$	93.085	93.550	95.715	95.856	96.759

**Table S2.** Calculated bond lengths and angles for BA cation at different pressures in Phase-I and Phase-II. Symmetry codes: (i) 0.5-x, -y, 0.5+z; (ii) 0.5-x, 1-y, 0.5+z; (iii) -0.5+x, y, 1.5-z; (iv) x, 0.5-y, 0.5+z; (v) 0.5+x, y, 1.5-z; (vi) -x, -0.5+y, 1.5-z; (vii) 1-x, 0.5+y, 1.5-z.

Distance (Å)	Phase-I		Phase-II		
	<b>0 GPa</b>	<b>0.78 GPa</b>	<b>1.12 GPa</b>	<b>2.90 GPa</b>	<b>4.68 GPa</b>
N1 <sup>vii</sup> —C1 <sup>vii</sup>	1.4831	1.4807	1.4802	1.4767	1.4721
C1 <sup>vii</sup> —C2 <sup>vii</sup>	1.4857	1.4842	1.4837	1.4805	1.4780
C2 <sup>vii</sup> —C3 <sup>vii</sup>	1.3875	1.3869	1.3870	1.3863	1.3844
C3 <sup>vii</sup> —C4 <sup>vii</sup>	1.3833	1.3831	1.3834	1.3823	1.3811
C4 <sup>vii</sup> —C5 <sup>vii</sup>	1.3835	1.3825	1.3827	1.3815	1.3811
C5 <sup>vii</sup> —C6 <sup>vii</sup>	1.3845	1.3843	1.3843	1.3825	1.3819
C6 <sup>vii</sup> —C7 <sup>vii</sup>	1.3821	1.3811	1.3813	1.3797	1.3782
C7 <sup>vii</sup> —C1 <sup>vii</sup>	1.3885	1.3887	1.3887	1.3879	1.3870
Angle (°)	Phase-I		Phase-II		
	<b>0 GPa</b>	<b>0.78 GPa</b>	<b>1.12 GPa</b>	<b>2.90 GPa</b>	<b>4.68 GPa</b>
∠N1 <sup>vii</sup> —C1 <sup>vii</sup> —C2 <sup>vii</sup>	112.060	111.842	111.580	110.637	110.271
∠C3 <sup>vii</sup> —C2 <sup>vii</sup> —C7 <sup>vii</sup>	119.225	119.340	119.478	119.626	119.814
∠C4 <sup>vii</sup> —C5 <sup>vii</sup> —C6 <sup>vii</sup>	120.121	120.267	120.367	120.511	120.555

**Table S3.** Calculated distances for nitrogen atom at different pressures in Phase-I and Phase-II. Symmetry codes: (i) 0.5-x, -y, 0.5+z; (ii) 0.5-x, 1-y, 0.5+z; (iii) -0.5+x, y, 1.5-z; (iv) x, 0.5-y, 0.5+z; (v) 0.5+x, y, 1.5-z; (vi) -x, -0.5+y, 1.5-z; (vii) 1-x, 0.5+y, 1.5-z.

Distance (Å)	Phase-I		Phase-II		
	0 GPa	0.78 GPa	1.12 GPa	2.90 GPa	4.68 GPa
N1 <sup>vii</sup> –I1 <sup>iv</sup>	3.6423	3.5984	3.5510	3.5064	3.4787
N1 <sup>vii</sup> –I1 <sup>ii</sup>	3.8923	3.8301	3.8535	3.7741	3.6714
N1 <sup>vii</sup> –I1 <sup>v</sup>	5.3427	5.2603	5.3918	5.2157	5.1614
N1 <sup>vii</sup> –I1 <sup>vii</sup>	3.6872	3.6093	3.6218	3.4871	3.3738
N1 <sup>vii</sup> –Pb1	4.5583	4.4745	4.3598	4.2346	4.0673
N1 <sup>vii</sup> –Pb1 <sup>i</sup>	5.5792	5.4860	5.4916	5.3761	5.2903
N1 <sup>vii</sup> –Pb1 <sup>vii</sup>	5.9689	5.8997	5.9493	5.7978	5.7019
N1 <sup>vii</sup> –Pb1 <sup>ii</sup>	4.5912	4.4900	4.4780	4.3689	4.2648

**Table S4.** The lattice parameters of  $(\text{BA})_2\text{PbI}_4$  from high-pressure synchrotron powder XRD experiments under different hydrostatic pressures from ambient to 4.68 GPa. The errors are given in the parentheses.

Sr	P	a	b	c	V	alpha	beta	gamma
	GPa	Å			Å <sup>3</sup>	Deg.		
1	0	9.1702(1)	8.7059(3)	28.8228(2)	2301.0(5)	90	90	90
2	0.16	9.1521(2)	8.6781(1)	28.6733(4)	2277.3(4)	90	90	90
3	0.31	9.1297(1)	8.6440(1)	28.4792(2)	2247.5(4)	90	90	90
4	0.5	9.1002(3)	8.6010(2)	28.2857(3)	2213.9(4)	90	90	90
5	0.78	9.0590(2)	8.5398(3)	28.0366(1)	2168.9(5)	90	90	90
6	1.12	9.0149(1)	8.5372(4)	27.7440(3)	2131.0(4)	88.98(1)	87.01(1)	91.63(1)
7	1.43	8.9973(2)	8.5336(4)	27.6118(2)	2114.5(3)	89.08(1)	86.56(3)	91.98(2)
8	1.73	8.9825(4)	8.5119(2)	27.5045(4)	2097.3(2)	89.22(2)	86.46(1)	92.07(2)
9	2.01	8.9569(2)	8.4900(2)	27.2983(3)	2069.4(5)	89.16(1)	86.48(2)	92.19(3)
10	2.4	8.9056(3)	8.4853(1)	27.0376(2)	2037.5(1)	89.42(3)	86.51(1)	92.30(2)
11	2.9	8.8483(2)	8.4367(2)	26.7383(3)	1990.8(3)	89.16(2)	86.77(2)	92.41(3)
12	3.11	8.8187(3)	8.4170(2)	26.6070(2)	1969.8(1)	89.07(1)	86.77(1)	92.38(1)
13	3.48	8.7425(4)	8.3815(4)	26.3588(3)	1927.0(3)	89.32(2)	86.89(2)	92.20(2)
14	3.81	8.7182(3)	8.3706(3)	26.2317(4)	1910.0(2)	89.37(1)	86.98(1)	92.23(3)
15	4.24	8.6970(2)	8.3533(2)	26.1406(1)	1894.9(1)	89.35(1)	87.01(1)	92.23(1)
16	4.68	8.6751(4)	8.3365(3)	26.0362(2)	1878.6(2)	89.34(3)	86.91(3)	92.20(2)